



^1H and ^{13}C NMR studies of glycine in anisotropic media: Double-quantum transitions and the effects of chiral interactions

Christoph Naumann, Philip W. Kuchel*

School of Molecular Bioscience, University of Sydney, Australia, NSW 2006, Australia

ARTICLE INFO

Article history:

Received 21 February 2011

Revised 18 April 2011

Available online 28 April 2011

Keywords:

Anisotropy

Chirality

z-Spectra

Double-quantum transition

NMR spectroscopy

ABSTRACT

The ^1H NMR spectrum of glycine in stretched gelatin gel and in cromolyn liquid crystal displays a well-resolved doublet due to ^1H – ^1H dipolar interaction. Multiple spectra were obtained within a wide range of offset frequencies of partially saturating radio-frequency (RF) radiation to generate steady-state irradiation envelopes or z-spectra of glycine. Maximal suppression of the doublet occurred when the irradiation was applied exactly at the centre frequency, between the two glycine peaks. This phenomenon is due to double-quantum transitions and is similar to our previous work on quadrupolar nuclei ^2H (HDO) and $^{23}\text{Na}^+$. When the ^{13}C isotopomer glycine-2- ^{13}C was used, the same effect was found in twice, split by $^1J_{\text{CH}} + 2D_{\text{CH}}$. Additional signals in ^1H and ^{13}C NMR due to prochiral–chiral interactions were found when glycine-2- ^{13}C was dissolved in chiral anisotropic gelatin and κ -carrageenan gels. The NMR spectra were successfully simulated assuming a $^2J_{\text{HH}}$ coupling constant of -16.5 Hz and two distinct dipolar coupling constants for the $^{-13}\text{CH}_2$ - group ($D_{\text{C,HA}}$ and $D_{\text{C,HB}}$).

© 2011 Elsevier Inc. All rights reserved.

1. Introduction

In this work we describe the application of magnetization transfer experiments on the methylene group of glycine ($\text{H}_3\text{N}^+-(^{13}\text{C})\text{CH}_2-\text{CO}_2^-$) involving magnetic **dipolar** interactions of the NMR-active spin-1/2 nuclei ^1H and ^{13}C . Unlabelled glycine dissolved in H_2O shows a single large resonance for its methylene protons in addition to the small ^{13}C – ^1H coupling of $^1J_{\text{C,H}} = 143$ Hz. The two methylene protons are enantiotopic but do not show any potential $^2J_{\text{H,H}}$ coupling due to their chemical-shift degeneracy. When glycine is dissolved in an anisotropic medium such as a liquid crystal [1] or stretched/compressed polymer gel [2], ^1H NMR peak splitting arises; a well-resolved doublet is seen. The extent of splitting corresponds to the residual dipolar coupling ($3D_{\text{AA}}$) [3]. Magnetization transfer experiments rely on the saturation of the magnetization of one spin population, and monitoring the effect on another. In our variant, radio-frequency (RF) radiation is applied at multiple frequency offsets across the whole NMR spectrum [4]. Plotting the peak integration for each spin as a function of frequency offsets yields the so called z-spectrum [5]. Previously we showed for **quadrupolar** NMR nuclei such as ^2H [6] and ^{23}Na [7] dissolved in stretched gelatin gel that the most marked suppression of the 1:1 doublet (for ^2H) or the 3:4:3 triplet (for ^{23}Na) occurs when

the irradiation is applied in the centre between the signals. We have shown that these phenomena are the result of multiple quantum transitions by providing a quantitative multiple quantum analysis for both quadrupolar nuclei [6,7]. Residual dipolar coupling (RDC) interactions in spin systems also lead to the formation of high-rank tensors that can be detected in NMR experiments by multiple quantum filtering [8]. These interactions are important in characterising ordered tissues such as cartilage and tendons, and potentially in other biological tissues such as muscle. In the present work we recorded z-spectra for glycine (an important amino acid constituent of connective tissue proteins) and its ^{13}C isotopomer glycine-2- ^{13}C . Since chirality is an integral part of biological tissues, we dissolved glycine in chiral gelatin and carrageenan gels [9,10], as well as into achiral cromolyn liquid crystal [11] for comparisons.

2. Results and discussion

2.1. ^1H NMR z-spectra of glycine and glycine-2- ^{13}C under isotropic and anisotropic conditions

Under isotropic conditions the z-spectra of 2 M glycine and 2 M glycine-2- ^{13}C dissolved individually into unstretched (isotropic) gelatin gels appeared as a broad singlet or doublet whose widths depended on the strength and duration of the radio-frequency radiation (Fig. 1a, black squares, Fig. 1b). When the irradiation power was increased, there were no new changes visible in the z-spectra, apart from an increase in broadening (Fig. 1b). Stretching

* Corresponding author. Present address: Singapore Bioimaging Consortium (SBIC), 11 Biopolis Way, #02-02 Helios, Singapore 138667, Singapore. Fax: +61 2 9351 4726.

E-mail address: philip.kuchel@sydney.edu.au (P.W. Kuchel).

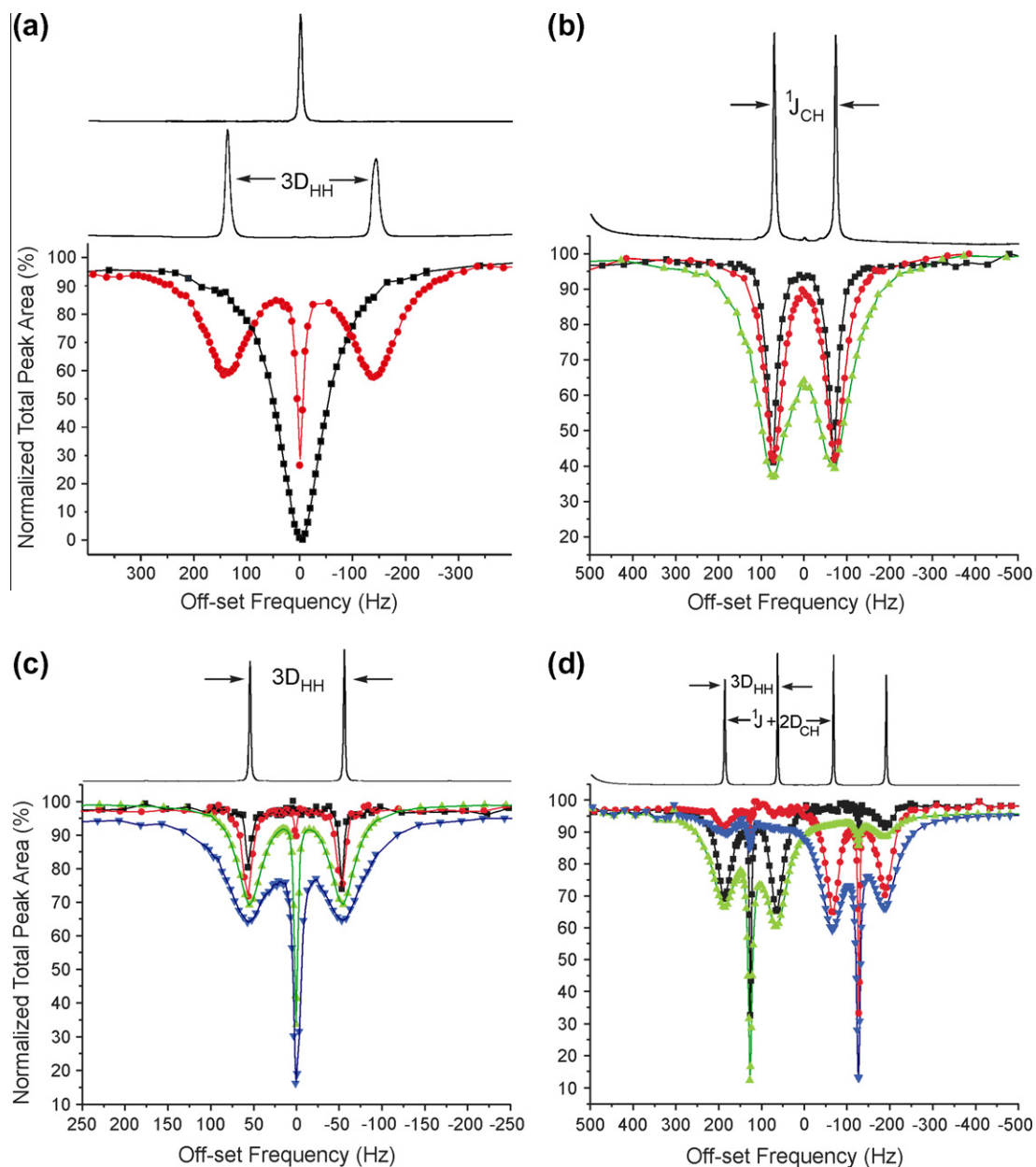


Fig. 1. ^1H NMR (400.13 MHz) steady-state irradiation envelopes (z-spectra; % integral of control spectrum) of glycine (a and c) and glycine- $2\text{-}^{13}\text{C}$ (b and d) under various isotropic (gelatin gel) and anisotropic (stretched gelatin gel, or cromolyn liquid crystal) conditions, and the effect of applying selective RF radiation with a range of magnitudes to the ^1H spins. The envelopes were derived by changing the offset frequency of the applied RF radiation and recording the corresponding ^1H NMR glycine signal integral. (a) 60% (weight for weight; w/w) gelatin gel made with 2 M glycine in D_2O ; black squares, unstretched (isotropic); red discs, stretched 1.4 times the original length for a glycine residual dipolar splitting ($3D_{\text{AA}}$) of 279 Hz and a D_2O residual quadrupolar splitting of 1050 Hz; glycine T_1 relaxation time was 1.0 s, the power attenuation of the steady-state irradiation was 55 dB (corresponding to an RF amplitude of ~ 34 Hz) and was applied for 5 s. (b) 100% w/w unstretched gelatin gel made with 2 M glycine- $2\text{-}^{13}\text{C}$ in D_2O ; T_1 relaxation time was 0.5 s, steady-state irradiation at each power level was applied for 5 s; black squares, 65 dB (10 Hz); red discs, 60 dB (19 Hz); green triangles, 55 dB (33 Hz). (c) 16% w/w cromolyn liquid crystal made with 0.3 M glycine in D_2O yielding a glycine residual dipolar coupling constant ($3D_{\text{AA}}$) of 110 Hz and a D_2O residual quadrupolar coupling constant of 193 Hz; T_1 relaxation time was 1.9 s, steady-state irradiation at each power level was applied for 8.5 s; black squares, 90 dB (0.8 Hz); red discs, 80 dB (2.6 Hz); green up-pointing triangles, 70 dB (8.2 Hz); blue down-pointing triangles, 65 dB (15 Hz). (d) 16% w/w cromolyn liquid crystal made with 0.3 M glycine- $2\text{-}^{13}\text{C}$ in D_2O yielding a glycine residual dipolar coupling constant ($3D_{\text{AA}}$) of 123 Hz, an RDC for the carbon–proton coupling of 111 Hz ($2D_{\text{AB}}$) and a D_2O quadrupolar splitting of 197 Hz; T_1 relaxation time was 1.3 s, steady-state irradiation at each power level was applied for 5 s; black squares (encompassing the sum of the two signals at higher frequencies) and red discs (sum of two lower frequency signals), 70 dB (8.2 Hz), green and blue triangles, 65 dB (15 Hz). (For interpretation of the references to colour in this figure legend, the reader is referred to the web version of this article.)

the two gels yielded anisotropic ^1H NMR spectra (bottom spectrum of Fig. 1a and d). Applying steady-state irradiation to obtain the z-spectrum under identical conditions to those used when the gel was isotropic, the resulting z-spectrum (Fig. 1a, red discs) looked strikingly similar to the z-spectra recorded for $^2\text{H}_2\text{O}$ in stretched gelatin [4]: the largest suppression of signal occurred exactly between the anisotropic methylene doublet in the form of a narrow

spike. The same phenomenon was recorded when glycine (or glycine- $2\text{-}^{13}\text{C}$) was dissolved in (achiral) cromolyn liquid crystal (Fig. 1c). In case of glycine- $2\text{-}^{13}\text{C}$ two spikes occurred, separated by $^1J_{\text{CH}} + 2D_{\text{CH}}$ (Fig. 1d). More powerful irradiation increased the depth of the spike (Fig. 1c). Clearly, the spike in the anisotropic z-spectra was due to double-quantum transitions, and did not depend on any (pro)chiral interactions.

However, in the case of glycine-2- ^{13}C in stretched gelatin, four additional small resonances were recorded in ^1H NMR spectra due to the interaction of the enantiotopic ^1H atoms, attached to the prochiral ^{13}C atom in the $^{-13}\text{CH}_2-$ group, with the chiral anisotropic matrix (Fig. 2). The additional resonances were caused by a difference in ordering in the two stereogenic C–H directions in a favourable chiral, orientated medium, changing the spin system from AX_2 to AXX' . The individual z-spectra obtained from the four major proton resonances showed, in addition to the central double-quantum spike (between signals 1 and 3, and 2 and 4), four smaller spikes on the resonances of the chirally induced signals. Each was correlated with one major signal, e.g., 1–1 s, 2–3 s (Fig. 2). The same information, but without evidence for the double-quantum transition, was obtained from a phase-sensitive 2D COSY experiment (Fig. 2).

2.2. ^{13}C NMR z-spectra of glycine-2- ^{13}C in chiral and achiral anisotropic media

The ^{13}C NMR spectrum of glycine-2- ^{13}C dissolved in cromolyn liquid crystal displayed the typical triplet of a $^{-13}\text{CH}_2-$ functionality with the scalar coupling enhanced by an RDC of the carbon and proton atoms of 111 Hz (Fig. 3a). Using chiral anisotropic media may introduce additional signals because of the interaction of the

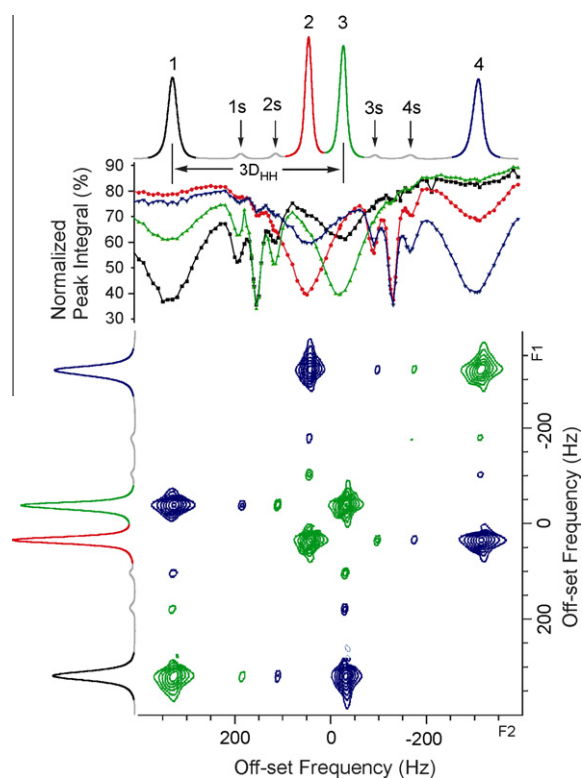


Fig. 2. ^1H NMR (400.13 MHz) steady-state irradiation envelope (z-spectra; % integral of control spectrum for the four major transitions 1–4). Steady-state irradiation at a power level of 55 dB (corresponding to an RF amplitude of ~ 34 Hz) was applied for 2.5 s and a 2D COSY correlation spectrum (phase-sensitive Bruker sequence cosydft) of glycine-2- ^{13}C was acquired under anisotropic conditions (stretched 100% w/w gelatin gel containing 2 M glycine-2- ^{13}C). Black squares, transition 1; red discs, transition 2; green up-pointing triangles, transition 3; blue down-pointing triangles, transition 4. Four additional transitions (labelled 1–4 s) can be seen due to the difference in ordering of the two stereogenic C–H directions of the prochiral glycine $^{-13}\text{CH}_2-$ group in a favourable chiral, orientated medium (changing the spin system from AX_2 to AXX') and were correlated to the major transitions by both z-spectra and the phase-sensitive COSY spectrum (green and dark-blue correlation signals correspond to opposing phases). (For interpretation of the references to colour in this figure legend, the reader is referred to the web version of this article.)

enantiotopic glycine methylene protons with the chiral matrix. This has been described before for the methylene protons of ethanol dissolved in the chiral liquid–crystal system poly- γ -(benzyl-L-glutamate)/deuterated chloroform (PBLG/ CDCl_3) [12]. In our case of glycine-2- ^{13}C , stretched and compressed gelatin gels, and a stretched κ -carrageenan gel, produced such an effect (Fig. 3b). Stretched ι -carrageenan gel although chiral as well did not yield this effect [10]. The additional signals could be correlated with the central resonance(s) by ^{13}C phase-sensitive COSY experiments. Integration confirmed a standard 1:2:1 triplet, and the corresponding z-spectra had the additional advantage of amplifying, the sometimes small, chirally induced signals (Fig. 3b). In cromolyn liquid crystals no additional signals were seen in the z-spectra, as expected for an achiral medium (Fig. 3a).

2.3. Simulating the chirally induced ^1H and ^{13}C NMR transitions

Glycine-2- ^{13}C showed four additional signals in ^1H NMR spectra, and two in ^{13}C NMR spectra, due to quasi diastereomeric complexation of the enantiotopic ^1H atoms attached to the prochiral ^{13}C atom in the $^{-13}\text{CH}_2-$ group, with the chiral anisotropic medium. The frequency and intensity of these signals depended on the extent and orientation of the anisotropic electric field-gradient tensor, but the main challenge was to model the spectral effects of the underlying chiral interaction [12]. Fig. 4 shows the eigenstate numbering scheme and idealized line spectra for an isotropic, anisotropic but achiral medium [13], and anisotropic and (favourable) chiral media. We made three assumptions in formulating this analysis: (a) the enantiotopic methylene protons have a $^2J_{\text{HH}}$ coupling constant of ~ 16 to 17 Hz that is normally “silent”. This estimate was based on literature values for the glycine methylene coupling constants measured in small peptides [14]. In addition, the coupling constant $^2J_{\text{H,D}}$ of monodeuterated glycine [15] is $|2.5|$ Hz [16], and when multiplied by the difference in the magnetogyric ratios ($\gamma_{\text{H}}/\gamma_{\text{D}} = 6.514$), the resulting $^2J_{\text{H,H}}$ is $|16.3|$ Hz. The sign of J_{gem} is often assumed to be negative, but $^2J_{\text{H,D}}$ can also be directly inferred (having a negative sign) from a linear plot of $^1(J + 2D)_{\text{C,H}}$ versus $^2(J + 2D)_{\text{H,D}}$ of monodeuterated glycine-2- ^{13}C dissolved in gelatin gel which is then stretched and compressed in various stages (data not shown, for a different case, this modulation of anisotropy yielding the absolute signs of scalar couplings has been done using variable angle spinning of a sample [17]); (b) the methylene protons in glycine-2- ^{13}C kept their chemical-shift degeneracy under anisotropic conditions. The ^1H NMR spectrum of glycine did not reveal any splitting based on chemical-shift differences; and (c) the residual dipolar coupling constant of the carbon–hydrogen bond ($2D_{\text{CH}}$) under (favourable) chiral, anisotropic conditions was no longer equally distributed, but two distinct dipolar coupling constants ($D_{\text{C,HA}}$, and $D_{\text{C,HB}}$) were postulated. Hence, by using these assumptions with Spinworks 3 software [18] we succeeded in simulating the NMR spectra (see experimental section for details). For stretched gelatin gels we found (by trial and error and selecting a $^2J_{\text{HH}}$ value of -16.5 Hz) a ratio for $D_{\text{C,HA}}$, and $D_{\text{C,HB}}$ of $\sim 2:3$ (Fig. 5a). To check the accuracy of our simulations we changed the orientation of the alignment of the sample (from a stretched to a compressed gel). When stretched gelatin gels are compressed, the signs of all dipolar coupling constants are switched, but not the sign of scalar coupling constants. This showed that the simulated spectra remained close to the experimental ones (Fig. 5b).

We further estimated the intensities and frequencies of the ^1H and ^{13}C NMR transitions of glycine-2- ^{13}C in stretched and compressed gelatin gels, based on the linear graph of D_{CH} versus D_{HH} for a compressed gelatin gel sample (Fig. 6a). In a first step, residual dipolar couplings ($2D_{\text{CH}}$) were estimated for a wide range of anisotropies, and after splitting the RDCs in a 2:3 ratio

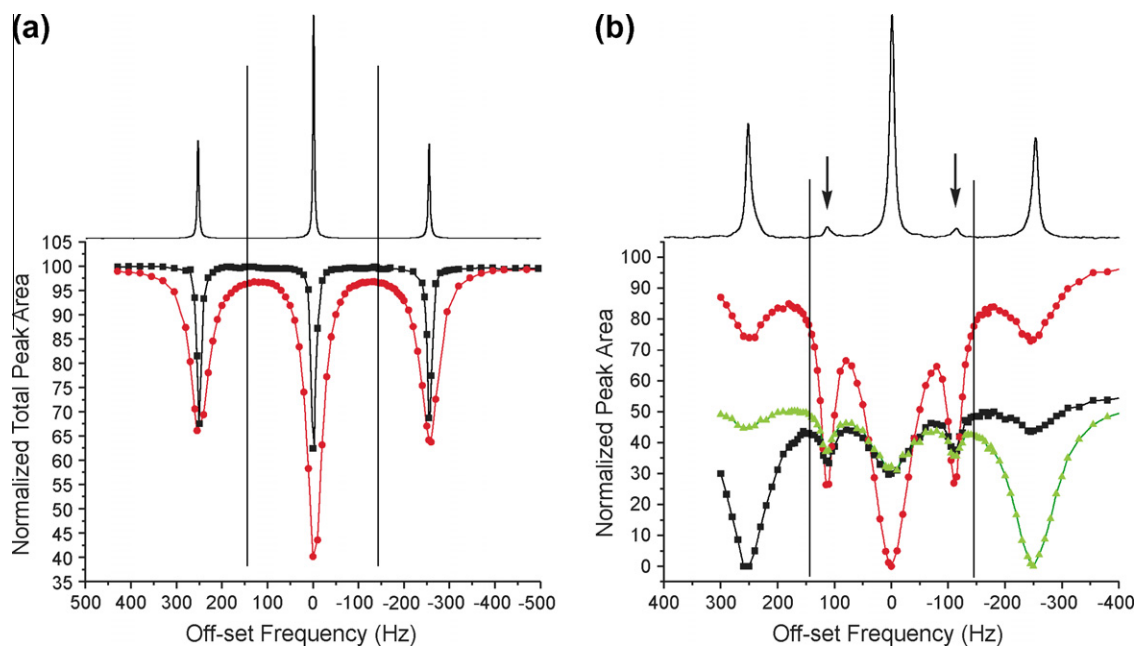


Fig. 3. ^{13}C NMR (100.61 MHz) steady-state irradiation envelopes (z-spectra; % integral of control spectrum) of glycine-2- ^{13}C under anisotropic (cromolyn liquid crystal and stretched gelatin gel) conditions. The envelopes were derived by changing the offset frequency of the applied RF radiation and recording the integral of the corresponding ^{13}C NMR glycine signal. (a) 16% w/w cromolyn liquid crystal made with 0.3 M glycine-2- ^{13}C in D_2O yielding a glycine RDC ($3D_{AA}$) of 123 Hz, an RDC for the carbon–proton coupling of 111 Hz ($2D_{AB}$) and a D_2O residual quadrupolar coupling constant of 197 Hz (the same sample as used for Fig. 1d); the T_1 relaxation time was 2.1 s, steady-state irradiation at each power level was applied for 8.5 s, and the normalized sum of the three signals is graphed; black squares, 85 dB (2.0 Hz); red discs, 70 dB (11 Hz). (b) 100% w/w stretched gelatin gel made with 2 M glycine-2- ^{13}C in D_2O yielding a glycine RDC ($3D_{AA}$) of 280 Hz, an RDC for the carbon–proton coupling of 112 Hz ($2D_{AB}$) and a D_2O residual quadrupolar coupling constant of 1018 Hz; glycine T_1 relaxation time was 0.5 s, the power attenuation of the steady-state radiation was 55 dB (22 Hz) and was applied for 2.5 s. The z-spectra of the three separate transitions are plotted individually: black squares, highest frequency transition; red discs, central transitions; green up-pointing triangles, lowest frequency transition. Two additional transitions, due to the difference in ordering for the two stereogenic C–H directions of the prochiral ^{13}C atom in the $^{-13}\text{CH}_2$ -group of glycine, in a favourable chiral, orientated medium (which changes the spin system from AX_2 to AXX') can be seen. (For interpretation of the references to colour in this figure legend, the reader is referred to the web version of this article.)

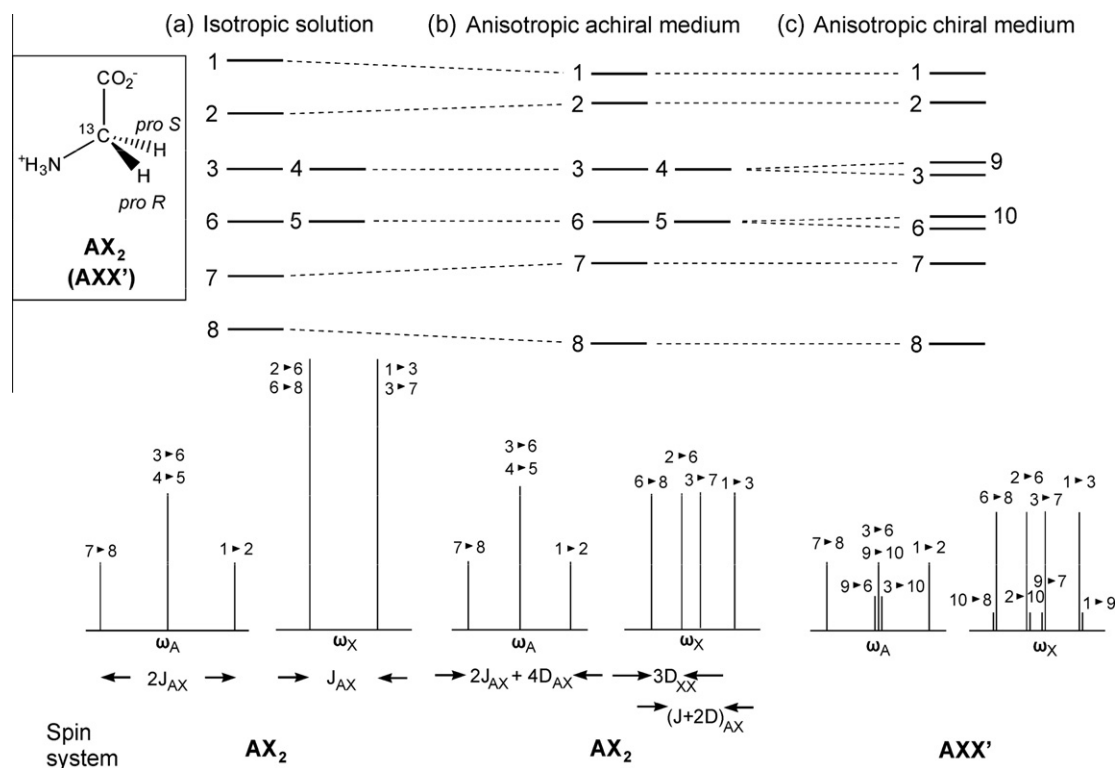


Fig. 4. Eigenstate numbering scheme and idealized line spectra for the three spin $^{13}\text{CH}_2$ (AX_2) system of glycine-2- ^{13}C in: (a) isotropic gel (unstretched gelatin gel) or solution; (b) anisotropic but achiral medium (e.g., cromolyn liquid crystals); and (c) anisotropic and favourable, chiral medium (e.g., stretched gelatin and κ -carrageenan gels). Part of this drawing was inspired by Fig. 1 in [13].

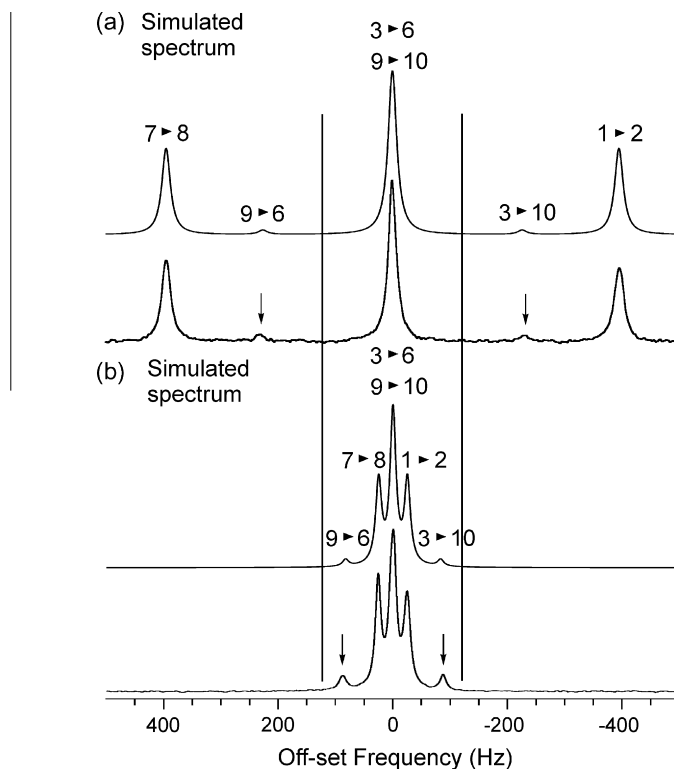


Fig. 5. Experimental and simulated ^{13}C NMR (100.61 MHz) spectra of glycine-2- ^{13}C incorporated in stretched (a) and compressed gelatin gel (b). The simulated spectra were based on the experimental data using Spinworks 3 [18] assuming $^1J_{\text{CH}} = 143.0$ Hz, $^2J_{\text{HH}} = -16.5$ Hz, and splitting the measured residual dipolar coupling of the carbon–hydrogen bond ($2D_{\text{CH}}$) in a 2:3 ratio, to generate two distinct dipolar coupling constants ($D_{\text{C,HA}}$, and $D_{\text{C,HB}}$). Positive D_{CH} values were assigned for stretched samples (together with positive D_{HH} values), and negative D_{CH} values for compressed samples (negative D_{HH}). The simulated spectra could be fine-tuned by varying slightly the above-mentioned 2:3 ratio (not done in this figure). The compressed gel was derived from the same stretched gelatin gel (150% w/w made with 0.47 M glycine-2- ^{13}C in D_2O , stretched 1.4 times the original length) by melting the anisotropy at 42 °C (15 min), and after cooling the sample to 15 °C, releasing the stretched tubing. The vertical bars denote the extent of the isotropic glycine-2- ^{13}C splitting, and the arrows on the experimental spectra point to the chirally induced ^{13}C transitions. The experimental data and parameter estimates used were, for: (a) $D_{\text{HH}} = 204.1$ Hz, $2D_{\text{CH}} = 252.0$ Hz, and display linewidth, 17.5 Hz and (b) $D_{\text{HH}} = -95.9$ Hz, $2D_{\text{CH}} = -117.9$ Hz, and display linewidth, 12.5 Hz.

($D_{\text{C,HA}} = 0.4 * 2D_{\text{CH}}$) spectra were simulated (Fig. 6). The modelling revealed two characteristic situations: one at $^1J_{\text{CH}} + 2D_{\text{CH}} = 123.7$ Hz (^{13}C splitting) when the central resonances disappeared and a doublet of a doublet arose in the ^{13}C NMR spectrum, and four sets of doublets appeared in the corresponding ^1H NMR spectrum, all of equal intensities; and the other at $^1J_{\text{CH}} + 2D_{\text{CH}} = 126.5$ Hz when the central resonances and the chirally induced resonances were of equal height/amplitude (see Fig. 6a). The former case occurred when D_{HH} was equal to $^2J_{\text{HH}}$ (-16.5 Hz), the later when $2D_{\text{CH}}$ equalled $^2J_{\text{HH}}$. The simulated data fitted closely to the experimentally derived plots of the frequencies of the transitions (Fig. 6b). The experimentally estimated minimum frequency difference, between the chirally induced ^{13}C signals and the central resonances based on the meeting point of the two linear fits of the data between the 25.1–121.7 Hz ^{13}C splitting, and 130.6–394.9 Hz, was 125.9 Hz. The minimum estimated from the simulation was at ~ 124.8 Hz, which was also indicated by the experimental data in the range of anisotropy achieved in the experiments (Fig. 6b inset). There is further scope for improving the simulations (“fine-tuning”) by varying the ratio between the two residual dipolar couplings, of the carbon–proton bond, but our focus was on a fast and easily replicable method.

3. Conclusions

We have shown that two, often invisible but potentially useful, NMR features of molecules, namely double-quantum transitions and “hidden” scalar coupling constants of commonly used dipolar (spin-1/2) nuclei can become visualisable by using (chiral) aniso-

tropic media. In our hands these phenomena were able to be recorded because of the large interaction between glycine and the anisotropic electric field-gradient tensor (shielding tensor) in stretched and compressed polymer gels, particularly in gelatin gels. The “hidden” scalar coupling of the enantiotopic methylene protons of glycine can only be measured by using chiral anisotropic media which in addition to their proven potential in enantiodiscrimination is another advantage of chiral alignment media [1,10,19]. The accuracy of estimates of values of any assumed NMR parameters can be quickly checked by simulating the experimental data from stretched and compressed states of the same sample; this is a reversible process which inverts the signs of dipolar coupling constants D while leaving the signs of the scalar coupling constants J unchanged. Glycine, as a common constituent of natural peptides and biomaterials may potentially be used as a marker for ordered systems. Beyond glycine, many protons in the side-chains of proteins are part of a methylene group, and the effects described here might also be applied to them. We posit that our findings are not simply of theoretical interest as they may be used in biological NMR to reduce spectral crowding, since ordered solvents/systems are widely used in NMR-based structure elucidation of biomolecules.

4. Experimental section

Gelatin gels (Gelita Asia Pacific, West Krugersdorp South Africa) and carrageenans gels (Sigma–Aldrich, St Louis, MO, USA) were prepared as described previously [9,10]. Cromolyn sodium salt (Aldrich) was dissolved in aqueous solutions of neutral pH

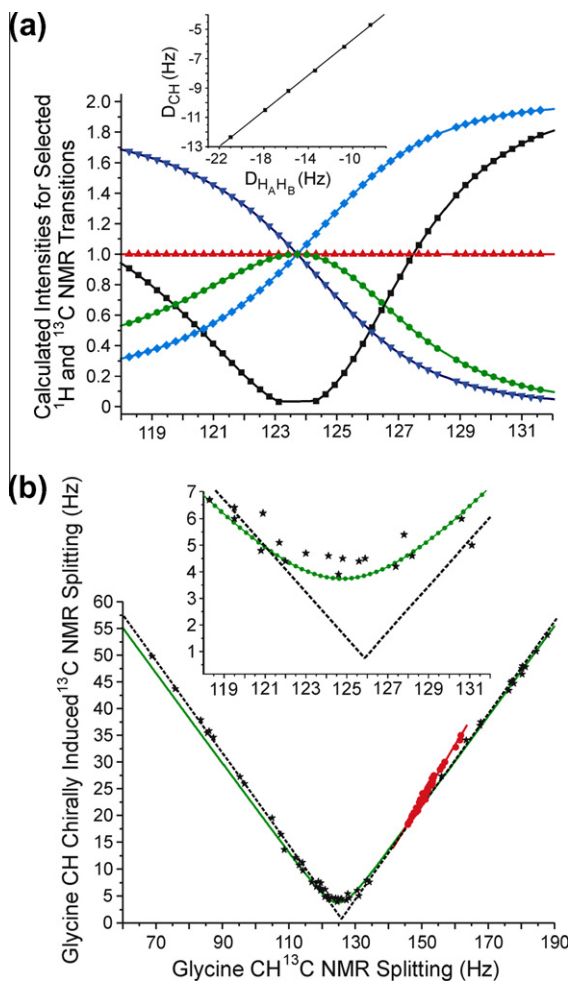


Fig. 6. Simulated (calculated) and experimentally derived (a) intensities and (b) frequencies for ¹H and ¹³C NMR transitions of glycine-2-¹³C in anisotropic gelatin gels (both stretched and compressed). ¹H and ¹³C NMR spectra (400.13 MHz for ¹H NMR, 15 °C) of a compressed gelatin gel (30% w/w) made with 0.42 M glycine-2-¹³C in D₂O were recorded at various stages of stretching and hence extents of anisotropy. The resulting linear fit to the data of glycine-2-¹³C D_{CH} versus D_{HH} (inset graph in a, $R = 0.9999$) was used to estimate RDCs over a wide, experimentally accessible anisotropic range from compressed to stretched stages (Fig. 4). Simulated spectra were then derived (Spinworks 3) [18] assuming $J_{C,H} = 143.0$ Hz, $J_{H,H} = -16.5$ Hz, and splitting the calculated residual dipolar coupling of the carbon–hydrogen bond ($2D_{CH}$) in a 2:3 ratio to generate two distinct RDCs ($D_{C,HA}$ and $D_{C,HB}$). Positive D_{CH} values were assigned for stretched samples (together with positive D_{HH} values), and negative D_{CH} values for compressed samples (negative D_{HH}). (a) Estimated intensities for ¹H and ¹³C transitions of glycine-2-¹³C: black squares, central ¹³CH transitions; green discs, chirally induced ¹³CH transitions; red up-pointing triangles, outer main ¹³CH transitions set to intensity 1.0; blue down-pointing triangles and light-blue diamonds, ¹H transitions (four each). (b) Graph of chirally induced glycine ¹³CH splitting versus glycine ¹³CH splitting. The inset is a magnified area of the main graph. Black stars denote the experimental data points from glycine-2-¹³C dissolved in anisotropic gelatin gels (of different gel concentrations) in the plotted range; red discs, glycine-2-¹³C dissolved in stretched κ-carrageenan gels (of different gel concentrations); green line or green discs (inset) show the simulated data; black dotted line, two linear fits of ¹³CH experimental data points: from 25.1–121.7 Hz ¹³CH splitting ($R = 0.9992$, 29 points), and between 130.6–394.9 Hz ¹³CH splitting ($R = 0.9993$, 45 points). (For interpretation of the references to colour in this figure legend, the reader is referred to the web version of this article.)

containing glycine or glycine-2-¹³C. The mixture was gently warmed to ~50 °C, transferred to a 5-mm NMR tube, warmed again, and stored at room temperature until measurement. Anisotropic gel samples were obtained by drawing molten gelatin or carrageenan solutions containing polar guest molecules in an elastic silicone rubber tube that allows (after the setting of the gel) the rapid and reversible adjustment of the degree of nuclear alignment

inside the NMR samples (starting from zero alignment) by merely stretching the rubber tube [9]. Stretched samples can be quickly and reversibly converted into compressed ones by melting the stretched gelatin gel by heating it at 37 °C, letting the gel reset by cooling, and then adjustably releasing the now isotropic sample; this compresses the gel and changes the sign of D . NMR spectra were recorded at 15 °C on a Bruker (Karlsruhe, Germany) 400 MHz vertical, wide-bore (Oxford Instruments, Oxford, UK) spectrometer. Simulated spectra were generated using Spinworks 3 software [18] assuming $J_{C,H} = 143.0$ Hz, $J_{H,H} = -16.5$ Hz, and splitting the measured or calculated residual dipolar coupling of the carbon–hydrogen bond ($2D_{CH}$) in a 2:3 ratio to generate two distinct RDCs ($D_{C,HA}$ and $D_{C,HB}$). Positive D_{CH} values were assigned for stretched samples (together with positive D_{HH} values), and negative D_{CH} values for compressed samples (negative D_{HH}). The simulations can be improved (“fine-tuned”) by varying the ratio between the two residual dipolar couplings of the carbon–proton bond. The linear fit of D_{CH} versus D_{HH} for a compressed gelatin gel sample used to calculate the graphs in Fig. 6 had the following equation: $y = 0.73 + 1.21x$.

Acknowledgments

The work was funded by an Australian Research Council Discovery Project grant to PWK. Dr Ann Kwan is thanked for assistance with the NMR spectrometer and Dr Uzi Eliav and Professor Gil Navon are thanked for valuable discussions.

References

- [1] (a) J.W. Emsley, J.C. Lindon, *NMR Spectroscopy Using Liquid Crystal Solvents*, Pergamon, Oxford, 1975; (b) C.F. Weise, J.C. Weisshaar, *J. Phys. Chem. B* 107 (2003) 3265–3277; (c) M. Sarfati, P. Lesot, D. Merlet, J. Courtieu *Chem. Commun.* (2000) 2069–2081; (d) D.H. Jones, S.J. Opella, *J. Magn. Reson.* 171 (2004) 258–269; (e) G. Kummerlöwe, B. Luy, *TrAC Trends Anal. Chem.* 28 (2009) 483–493.
- [2] (a) J.J. Chou, S. Gaemers, B. Howder, J.M. Louis, A. Bax, *J. Biomol. NMR* 21 (2001) 377–382; (b) P.W. Kuchel, B.E. Chapman, N. Müller, W.A. Bubba, D.J. Philp, A.M. Torres, *J. Magn. Reson.* 180 (2006) 256–265; (c) G. Kummerlöwe, F. Halbach, B. Laufer, B. Luy, *Open Spectrosc. J.* 2 (2008) 29–33.
- [3] M.H. Levitt, *Spin Dynamics: Basics of Nuclear Magnetic Resonance*, second ed., Wiley & Sons, 2008.
- [4] P.W. Kuchel, C. Naumann, *J. Magn. Reson.* 192 (2008) 48–59.
- [5] J. Grad, R.G. Bryant, *J. Magn. Reson.* 90 (1990) 1–8.
- [6] U. Eliav, C. Naumann, G. Navon, P.W. Kuchel, *J. Magn. Reson.* 198 (2009) 197–203.
- [7] B.E. Chapman, C. Naumann, D.J. Philp, U. Eliav, G. Navon, P.W. Kuchel, *J. Magn. Reson.* 205 (2010) 260–268.
- [8] For instance see J. Tang, A. Pines, *J. Chem. Phys.* 72 (1980) 3290–3297.
- [9] C. Naumann, P.W. Kuchel, *J. Phys. Chem. A* 112 (2008) 8659–8664.
- [10] (a) C. Naumann, P.W. Kuchel, *Chem. Eur. J.* 15 (2009) 12189–12191; (b) C. Naumann, P.W. Kuchel, *Polym. Chem.* 1 (2010) 1109–1116.
- [11] (a) D. Goldfarb, M.M. Labes, Z. Luz, R. Poupko, *Mol. Cryst. Liq. Cryst.* 87 (1982) 259–279; (b) D. Goldfarb, M.E. Moseley, M.M. Labes, Z. Luz, *Mol. Cryst. Liq. Cryst.* 89 (1982) 119–135.
- [12] (a) D. Merlot, A. Loewenstein, W. Smadja, J. Courtieu, P. Lesot, *J. Am. Chem. Soc.* 120 (1998) 963–969; (b) C. Aroulanda, D. Merlet, J. Courtieu, P. Lesot, *J. Am. Chem. Soc.* 123 (2001) 12059–12066.
- [13] L.G. Werbelow, D.M. Grant, E.P. Black, J.M. Courtieu, *J. Chem. Phys.* 69 (1978) 2407–2419.
- [14] M. Barfield, V.J. Hruby, J.-P. Meraldi, *J. Am. Chem. Soc.* 98 (1976) 1308–1314.
- [15] Monodeuterated glycine-2-¹³C was prepared (together with bisdeuterated glycine-2-¹³C) according to S. Yamada, C. Hongo, R. Yoshioka, I. Chibata, *J. Org. Chem.* 48 (1983) 843–846. The couplings $J_{C,H}$ and $J_{H,D}$ were extracted from ¹H NMR spectra at 15 °C and 400.13 MHz.
- [16] A. Rios, J.P. Richards, *J. Am. Chem. Soc.* 119 (1997) 8375–8376.
- [17] M. Edgar, J.W. Emsley, M.I.C. Furby, *J. Magn. Reson.* 128 (1997) 105–113.
- [18] Spinworks 3 by Kirk Marat, University of Manitoba, Canada.
- [19] (a) A. Marx, V. Schmidts, C.M. Thiele, *Magn. Reson. Chem.* 47 (2009) 734–740; (b) C.M. Thiele, W.C. Pomerantz, N.L. Abbott, S.H. Gellman, *Chem. Commun.* 47 (2011) 502–504.